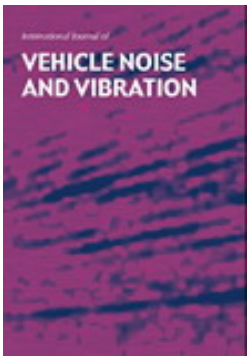

International Journal of Vehicle Noise and Vibration

ISSN online: 1479-148X - ISSN print: 1479-1471
https://www.inderscience.com/ijvnv

Complex eigenvalue analysis of aluminium composites disc brake with damping

P.S. Sree Ganesh, S. Vengatesan

DOI: 10.1504/IJVNV.2022.10053243

Article History:

Received:	10 May 2022
Accepted:	09 October 2022
Published online:	10 April 2023

Complex eigenvalue analysis of aluminium composites disc brake with damping

P.S. Sree Ganesh

Department of Automobile Engineering,
College of Engineering and Technology,
SRM Institute of Science and Technology,
Chengalpattu – 603203, India
Email: ps2483@srmist.edu.in

S. Vengatesan*

Department of Mechanical Engineering,
College of Engineering and Technology,
SRM Institute of Science and Technology,
Chengalpattu – 603203, India
Email: vs2725@srmist.edu.in
and
Renault Nissan Technology and Business Centre India,
Chengalpattu, Tamil Nadu, India
Email: vengatesan.subramanian@rntbci.com
*Corresponding author

Abstract: The behaviour of brake squeal is analysed using a complex eigenvalue method with damping for grey cast iron (GCI) and two types of aluminium matrix composite considering different distributions of SiC particles in the aluminium matrix. The influence of the friction between disk brake and brake pad, and the behaviour of the logarithmic decrement and its stability are studied under high frequency range and the influence on brake squeal. The simulation results show that the relationship between friction factor and damping frequency plays a vital role in brake squeal when the bending mode exists in lateral direction. The analysis helps us to choose the appropriate material combination to suppress the brake squeal phenomenon in major engineering applications.

Keywords: disc brake squeal; modal analysis; metal matrix composites; monomodal; bimodal.

Reference to this paper should be made as follows: Ganesh, P.S.S. and Vengatesan, S. (2023) 'Complex eigenvalue analysis of aluminium composites disc brake with damping', *Int. J. Vehicle Noise and Vibration*, Vol. 19, Nos. 1/2, pp.15–31.

Biographical notes: P.S. Sree Ganesh received his Bachelor's in Automobile Engineering at SRM Institute of Science and Technology, KTR Campus. Currently, he is pursuing his Masters in Automotive Engineering at Politecnico di Torino, Turin, Italy.

S. Vengatesan received his Master's in Engineering Design from College of Engineering Guindy, Anna University and pursuing his PhD in New numerical technique in Finite element method for structural mechanics using polygonal elements at SRM Institute of Science and Technology, KTR Campus. Currently, he is working as a Senior Engineer in RNTBCI, specifically focusing on brake system calculations.

1 Introduction

NVH is considered to be among the top attributes by which one can determine the quality of a vehicle. Qatu (2012) has made a summary about the main NVH sources in automobiles. These include powertrain, tyres, chassis, brakes, etc. One of the critical tasks in automobiles manufacturing is to control NVH to the minimum level according to the government noise and pollution control norms (Nouby et al., 2011). A detailed study has been conducted by Qatu et al. (2009), where NVH has been categorised into interior and exterior NVH. All NVH sources like engine, tyres, brakes, are treated as interior NVH. The noises generated while driving, their impact on the environment and the different policies in place, have been mentioned in the exterior type NVH.

While designing disc brakes, the brake squeal is one of the significant factors that need to be considered. Increase in squeal leads to the inconvenience of customers and decreases the efficiency and life span of the braking system, particularly in passenger cars. Among the various types of noises which occur while braking, squeal is the most common and is difficult to avoid, because it falls in category of high frequency noises (more than 1 kHz), to which the human ear is most sensitive (Triches et al., 2004). As there is no definite reason to explain the occurrence of squeal, several analytical, experimental, and numerical techniques have been used to analyse and reduce disc brake squeal, with each approach having limitations, advantages, and disadvantages. Kinkaid et al. (2003) gave an elaborated review on brake squeal and stated as "despite a century of developing disc brake systems, disc brake squeal remains a largely unresolved problem".

The experimental testing and verification has been done by many researchers to control the brake squeal. The earlier work is Mills (1938) and followed by Fosberry and Holubecki (1959, 1961) and few of them were correlated with experimental results. Quite a few studies have been carried out to compare the efficiency of experimental procedures and numerical methods in predicting disc brake squeal (Kadu and Vivekanandan, 2015). The effect of modifying the shapes of the brake pads on squeal by making them symmetric, has also been studied (Pan et al., 2021). It has been found that physical parameters and material properties of the rotor/ drum can influence the amount of squeal generated. The properties examined in the review are Young's modulus of the rotor and back plate, temperature, brake pressure, friction coefficient, contact area of the pads and rotational velocity (Miranda et al., 2020).

In 2001, Denou and Nishiwaki investigated the squeal phenomenon on the modified disc brake. The correlation between the change in contact area and its influences is addressed very extensively.

The impact of using fibrous materials like aramid or asbestos has also been studied (Idusuyi et al., 2014). In the recent research work (Pan et al., 2021), the squeal between

symmetrical and asymmetrical calliper has been compared with experimental results. The experimental investigation on brake squeal is non-trivial since its randomness behaviour and the results are particularly for specific experimental setup (Giannini et al., 2006). Adebisi et al. (2011) presented the friction induced noise phenomenon and brake squeal mechanism with experimental and CAE analysis. The CAE results are very robust compared to the experimental results. The complex eigenvalue analysis has been done on disc brake squeal using ABAQUS by Liu et al. (2007). Where the authors identified the significant bending modes causes for disc brake squeal and it can be reduced by modifying the shape of the disc brake, using damping material or decreasing the friction coefficient for isotropic material.

The computational simulation study on squeal noise of the disc brake rotor with frictional condition of the pads along with damping factor is not addressed till now to the authors' knowledge for composite material. In this work, the attempt has been taken to find the behaviour of the brake rotor with grey cast iron (GCI) and aluminium composite material for the squeal induced frequency and its influence on stability and logarithmic decrements.

The following contents are arranged as in Section 2 the methodology followed for computational study has been explained in detail. In Section 3, the materials used for the study and followed by results of the simulation in Section 4. The summary of the results and its inference are discussed in Section 5.

2 Methodology

2.1 Geometry description

The 3-dimensional CAD model of the rotor was modelled in SOLIDWORKS. In contrast to solid discs, ventilated rotors are dissipating more heat, which can be in excess of 500°C in some situations. This increases braking efficiency and minimises the risk of brake fade; a drawback usually associated with solid rotors for the same conditions. The model used in our study, as depicted in Figure 1, has a diameter of 240 mm containing diameter of 4 mm circular slots, along with pads having 50 mm width, covering an arc of 80°.

2.2 Complex eigenvalue extraction

Subspace projection method is used in complex eigenvalue extraction, for that natural frequency is required to compute the subspace. The basic governing equation to extract the natural frequency is as in equation (1).

$$M\ddot{x} + C\dot{x} + Kx = 0 \tag{1}$$

The modified governing equation with friction factor can be written as in equation (2).

$$\left(\mu^2 M + \mu C + K\right)\Phi = 0 \tag{2}$$

The μ and ϕ are eigenvalue and eigenvector respectively, it may be complex number. To execute the complex eigenvalue analysis by, neglecting the unsymmetric contribution in

the stiffness matrix and ignoring the damping matrix to get the symmetric system. After getting the eigenvectors, the matrices are projected on the subspace on N eigenvectors.

$$\begin{aligned} \boldsymbol{M}^* &= [\phi_1, \ldots, \phi_N]^{\mathrm{T}} \boldsymbol{M} [\phi_1, \ldots, \phi_N] \\ \boldsymbol{C}^* &= [\phi_1, \ldots, \phi_N]^{\mathrm{T}} \boldsymbol{C} [\phi_1, \ldots, \phi_N] \\ \boldsymbol{K}^* &= [\phi_1, \ldots, \phi_N]^{\mathrm{T}} \boldsymbol{K} [\phi_1, \ldots, \phi_N] \end{aligned} \tag{3}$$

Then the projected complex eigenproblem becomes in simplified form

$$\left(\mu^2 \boldsymbol{M} + \mu \boldsymbol{C} + \boldsymbol{K}\right) \boldsymbol{\Phi} = 0 \tag{4}$$

The eigenvectors can be obtained by

$$\phi = [\phi_1 \ldots \phi_N]^T * \phi^* \tag{5}$$

A more detailed description of the algorithm may be found in ABAQUS study material. The complex eigenvalue ϕ, can be expressed as $\mu = \alpha + \mathrm{i}\ \omega$, real part of μ, Re(μ), indicating the stability of the system, imaginary part of μ, Im(μ), indicating the mode frequency of the system. The displacement of the system expressed as follows in generalised form

$$x = A\mathrm{e}^{\mu t} = \mathrm{c}^{\alpha t} \left(A_1 \cos \omega t + A_2 \sin \omega t\right) \tag{6}$$

The stability of the system and damping factors are analysed using these formulation and based on the values the influence on the brake squeal is predicted.

Figure 1 Rotor model, (a) isometric view (b) rotor and slot dimensions

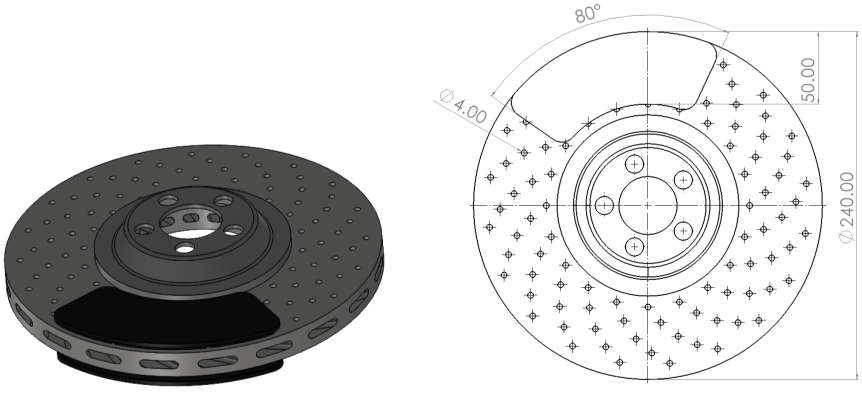

(a) (b)

2.3 Simulation conditions

The geometry is imported to ANSYS workbench with model analysis module. The material properties are defined as in Table 2. The fine mesh is considered for the analysis to avoid the convergence issue.

The friction induced dynamic stability is the cause of brake squeal in the disc brake. There are two methods to inspect the brake squeal as follows:

- complex eigenvalue analysis (CEA)
- transient dynamic analysis (TDA).

The finite element method is one of the most reliable methods to analyse complex eigenvalue modal analysis, where it calculates friction coupling by static dynamic analysis. The TDA is computationally expensive compared to the complex eigenvalue analysis (Liu et al., 2007). After which the complex eigenvalues are extracted from the simulation, where the information about the stability of the system, unstable modes and the mode shape can be interpreted. This approach is computationally fast and effective, as it computes all the unstable modes. However, it should be noted that CEA does not take the nonlinear effects and uniform contact into consideration (Nilman, 2018). The extracted complex eigenvalues are in the form of:

$$\lambda = \sigma + j\omega$$

where λ is the value extracted, σ is the real part denotes the stability of the system and ω is the imaginary part containing the corresponding damping frequency. The real parts of the eigenvalues dictate the stability (or lack of it) of the system. If the real part of an eigenvalue is positive, the corresponding imaginary part was thought to be a possible squeal frequency (Pan et al., 2021).

TDA is an explicit approach that does not need a convergent solution before attempting the next time step. In complex eigenvalue analysis, the squeal is treated as a vibration problem in the time domain and unstable frequencies can be predicted (Miranda et al., 2020). TDA is not used often as it takes a long time to compute and does not give any information regarding the mode shapes. Information about the displacement, acceleration, velocity, force and area of the contact during system vibration can be obtained from this analysis (Nilman, 2018).

- direct input: the stiffness coefficient and mass coefficient need to be given directly into the solver
- damping vs. frequency: the stiffness coefficient and mass coefficient are calculated from the user defined values of damping ratio and frequency.

Damping vs. frequency method was selected for this simulation, as stiffness coefficient and mass coefficient need not be provided as boundary conditions. These values are calculated by the solver during simulation. According to Rayleigh damping, damping ratio depends on two constants α and β.

$$\begin{aligned}\alpha &= \frac{2\omega_i\omega_j}{\omega_j^2 - \omega_i^2}\left(\omega_j\xi_i - \omega_i\xi_j\right)\\ \beta &= \frac{2}{\omega_j^2 - \omega_i^2}\left(\omega_j\xi_j - \omega_i\xi_i\right)\\ \xi &= \frac{\alpha}{2\omega_i} + \frac{\beta\omega_i}{2}\end{aligned} \tag{7}$$

In the above equations, ξ_i and ξ_j are the damping ratios corresponding to the natural circular frequencies ω_i and ω_j. It is assumed that the sum of alpha and beta remains constant over a wide range of frequencies.

Figure 2 Materials for matrix and reinforcement (see online version for colours)

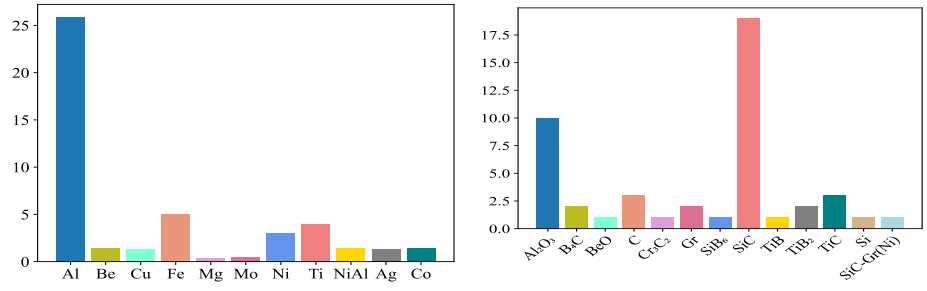

(a) (b)

In order to add damping to a system, the Coriolis effect was set as ON in the modal system. Damping ratio was fixed at 0.005 and the frequency values were varied from 1,000 Hz to 7,000 Hz, in increments of 2,000 Hz. Frictional type of contact was specified at the rotor-pad interface, having coefficient of friction as 0.2. The constraints applied on the model are depicted in Figure 3. Later the friction coefficient values are varied to find the influence of friction coefficient on brake squeal. The coefficient was assigned the values of 0.1, 0.2, 0.3 and 0.4, keeping the frequency constant at 7,000 Hz. Other parameters remained the same.

Figure 3 Constraints on the model (see online version for colours)

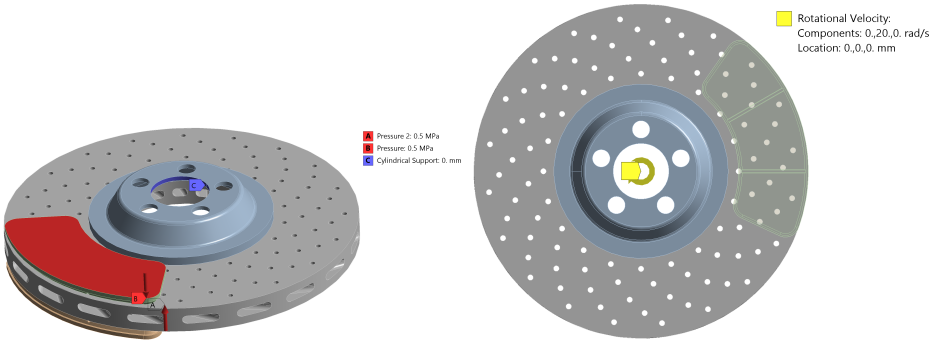

The number of modes was set to six and the values of damping frequency, stability (Hz), modal damping ratio and logarithmic decrement were computed for all the modes of each material, at the four frequencies.

3 Material selection

As GCI is frequently used to manufacture brake rotors commercially. For the selection of the composite materials, two types of AMC were chosen, namely monomodal and bimodal. By properly mixing four distinct particle sizes of the SiC reinforcement with sizes 10, 54, 86 and 146 micrometres, in such a way that the combinations yielded porous bodies with monomodal, bimodal, trimodal, and quatrimodal size distribution,

with 1, 1:5, 1:1:4 and 1:1:1:3 particle size ratios, respectively (Montoya-Dávila et al., 2010). Of the four AMCs, monomodal and bimodal were selected for the analysis.

Table 1 Chemical composition (wt%) and molar ratio Si/Mg of the aluminium alloy used

Alloy contents	*Al*	*Mg*	*Si*	*Fe*	*Mn*	*Cu*	*Si/Mg*
Wt (%)/molar ratio	Balance	13.29	1.78	0.626	0.118	0.055	0.116

The density of the composites increases with an increase in particle size distribution from monomodal to bimodal, this is due to better filling of porous preforms by aluminium alloy due to decrease in pores sizes, as in Table 2. Pore size decreases by approximately 65% from monomodal to bimodal. The values of Young's modulus are augmented with increase in the particle size distribution, the reinforcement endures and transmits load through the metallic matrix, like shown in Table 2 (Montoya-Dávila et al., 2010).

Aluminium and SiC are the most commonly used matrix materials and reinforcement materials respectively, as shown in Figure 2 (Adebisi et al., 2011). Aluminium alloys are selected for MMCs due to their high ductility, high strength-to-weight ratio, excellent wear resistance, and good thermal and electrical characteristics (Miracle, 2005; Sadagopan et al., 2018). The chemical composition of the aluminium alloy used in the AMC is given in Table 1 (Montoya-Dávila et al., 2010). An increase in both hardness and impact strength of the composite is observed, with an increase in weight percentage of SiC up to 25%. Beyond which, the hardness trend started decreasing as SiC particles interacted with each other leading to the clustering of particles and consequently settling down (Singla et al., 2009).

Table 2 Material properties of GCI, monomodal and bimodal

S. no.	*Material*	*Density (kg/m³)*	*Young's Modulus (GPa)*	*Poisson's ratio*	*Porosity (%)*
1	Grey cast iron	7150	101.50	0.29	-
2	Monomodal	2840	185.39	0.23	4.42 ± 0.022
3	Bimodal	2920	190.09	0.23	1.48 ± 0.012

Source: Montoya-Dávila et al. (2010)

The three materials were defined in the engineering data section providing density and isotropic elasticity. Pads were treated as an orthotropic material. The equivalent material proprieties for the aluminium composite are taken from the reference for simulation.

4 Results and discussion

The eigenvalue analysis is carried out with three different material properties, where the GCI is considered to be isotropic and homogeneous to compare the results with composite disc brake. The remaining two materials are based on the dispersion of silicon particle in the aluminium matrix, called as monomodal and bimodal material based on the distribution ratio of silicon particles. The equivalent material properties

(Montoya-Dávila et al., 2010) are considered for the simulation of aluminium- silicon composite disc brake rotor.

The damping frequency is varied between 1,000 Hz to 7,000 Hz based on the existing literature. The first six modes are taken for the comparison purpose and tabulated in Table 3.

Figure 4 Comparison with damping frequency (Hz) (see online version for colours)

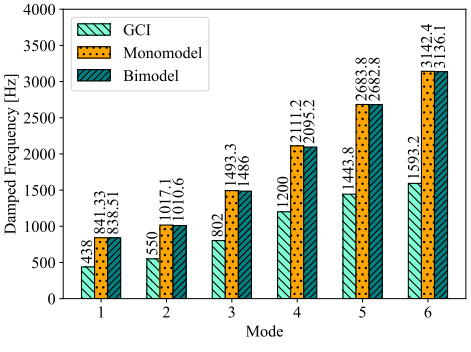

Table 3 Comparison of damping frequency and stability of the cast iron, monomodal and bimodal with damping

Mode	*Damping frequency [Hz]*			*Stability [Hz]*		
	Cast iron	*Monomodal*	*Bimodal*	*Cast iron*	*Monomodal*	*Bimodal*
1	438	841	838	–0.119	–0.4425	–0.4397
2	549	1,017	1,010	–0.179	–0.5847	–0.5757
3	802	1,493	1,486	–0.310	–1.1916	–1.1852
4	1,202	2,111	2,095	–0.850	–2.3257	–2.2884
5	1,443	2,683	2,682	–1.28	–4.7574	–4.7566
6	1,593	3,142	3,136	–1.55	–6.2524	–6.2298

Table 4 Comparison of damping ratio and logarithmic decrement for cast iron, monomodal and bimodal of aluminium alloy damping

Mode	*Modal damping ratio*			*Logarithmic decrement*		
	Cast iron	*Monomodal*	*Bimodal*	*Cast iron*	*Monomodal*	*Bimodal*
1	2.70E-04	5.26E-04	5.24E-04	–1.70E-03	–3.30E-03	–3.30E-03
2	3.26E-04	5.75E-04	5.70E-04	–2.05E-03	–3.61E-03	–3.58E-03
3	3.87E-04	7.98E-04	7.98E-04	–2.43E-03	–5.01E-03	–5.01E-03
4	7.07E-04	1.10E-03	1.09E-03	–4.44E-03	–6.92E-03	–6.86E-03
5	8.89E-04	1.77E-03	1.77E-03	–5.59E-03	–1.11E-02	–1.11E-02
6	9.74E-04	1.99E-03	1.99E-03	–6.12E-03	–1.25E-02	–1.25E-02

From the results of damping frequency, on comparing GCI, monomodal and bimodal, the frequency values are shifted drastically for the silicon reinforced aluminium disc. During the higher modes its moving exponentially approximately 50% compared to the GCI disc brake. The negative stability values indicate the stability modes of the disc

brake. The positive value of the stability leads to unstable modes and reason for squeal noise in the disc brake (Liu et al., 2007).

Figure 5 Comparison of logarithmic decrement of GCI at different modes in the frequency range of 1,000 Hz to 7,000 Hz (see online version for colours)

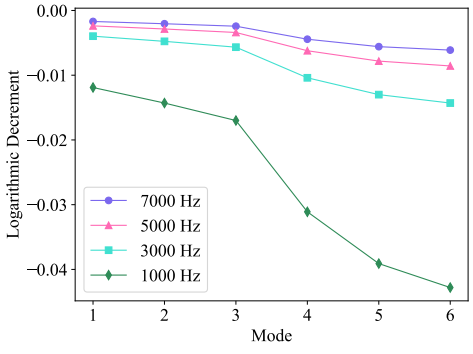

Figure 6 Comparison of logarithmic decrement of monomodal at different modes in the frequency range of 1,000 Hz to 7,000 Hz (see online version for colours)

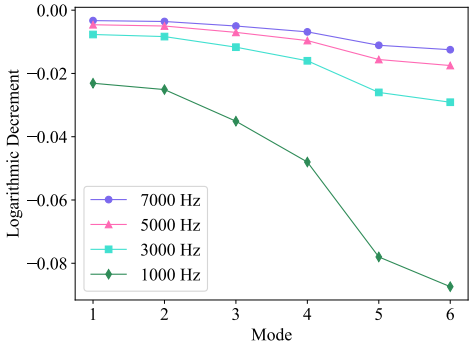

Figure 7 Comparison of logarithmic decrement of bimodal at different modes in the frequency range of 1,000 Hz to 7,000 Hz (see online version for colours)

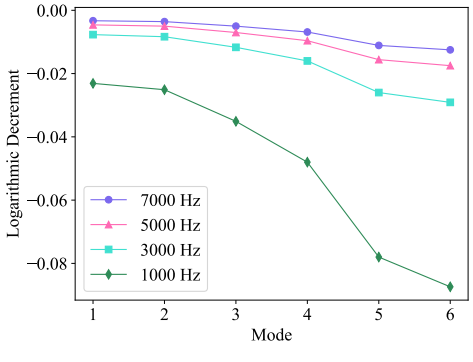

The modal damping ratio and logarithmic decrement are tabulated in Table 4 for the same six modes mentioned in Table 3.

From the results of the complex eigenvalue analysis it is seen that the damping ratio values for monomodal and bimodal are almost the same compared to the GCI. The positive damping ratio values indicate the system is stable and vice-versa (Liu et al., 2007). To give the better visibility on change in the frequency value the graph between damping frequency vs. mode was plotted, as in Figure 4.

The influence of the frequency on the logarithmic decrement plotted for GCI, monomodal and bimodal in Figures 5, 6 and 7. The plot reveals the influence of the frequency value for different modes: at higher frequency the decrements in amplitude is very high and with increase in higher modes the lower frequency condition the rate of decrement is much less.

For the same input frequency, the logarithmic decrements values are compared for GCI, monomodal and bimodal as in Figure 8. At the maximum frequency the monomodal and bimodal are following the same trend and GCI has higher rate of decrements compared to the aluminium composite.

Figure 8 Comparison between different materials at damped frequency of 7,000 Hz (see online version for colours)

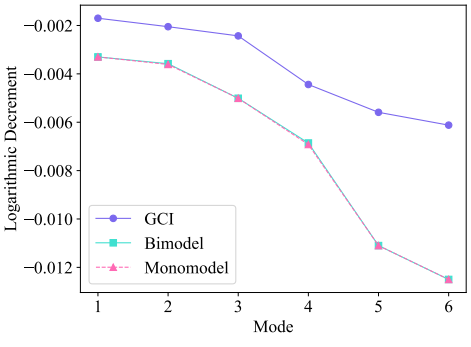

The influence of the friction coefficient between the brake disc and pad with varying values as 0.1, 0.3, 0.4. For each material, the simulation is carried out and comparison is plotted for better understanding. For the GCI, monomodal and bimodal the values are tabulated with change in friction coefficient as in Tables 5, 6 and 7, respectively.

Table 5 The damping frequency and stability for the different friction coefficients for grey cast iron

Mode	*Damping frequency [Hz]*			*Stability [Hz]*		
	0.1	*0.3*	*0.4*	*0.1*	*0.3*	*0.4*
1	427.18	446.9	453.69	–0.11535	–0.1217	–0.12454
2	545.95	551.93	553.89	–0.17624	–0.18048	–0.18159
3	731.92	852.35	890.41	–0.27863	–0.3441	–0.37628
4	1,196.4	1,207	1,210.7	–0.84205	–0.85766	–0.86406
5	1,428.6	1,456.5	1,467.7	–1.2843	–1.2853	–1.288
6	1,568.4	1,613.7	1,631.1	–1.5357	–1.5713	–1.5909

Table 6 The damping frequency and stability for the monomodal material with varying friction coefficient

Mode	*Damping frequency [Hz]*			*Stability [Hz]*		
	0.1	*0.3*	*0.4*	*0.1*	*0.3*	*0.4*
1	824.91	854.08	864.55	–0.43367	–0.45116	–0.45911
2	1,008.7	1,022.4	1,026.3	–0.57244	–0.59269	–0.59834
3	1,399.6	1,563	1,617.8	–1.1197	–1.2718	–1.3491
4	2,100	2,120.2	2,128	–2.3154	–2.3365	–2.3468
5	2,675.5	2,690.9	2,697.2	–4.7542	–4.7607	–4.7638
6	3,122.3	3,157.4	3,169.5	–6.2055	–6.2932	–6.3269

Table 7 The damping frequency and stability for bimodal material with different friction coefficient

Mode	*Damping frequency [Hz]*			*Stability [Hz]*		
	0.1	*0.3*	*0.4*	*0.1*	*0.3*	*0.4*
1	822.38	851.05	861.37	–0.43106	–0.44819	–0.45598
2	1,002.1	1,015.9	1,019.8	–0.56359	–0.58371	–0.58939
3	1,394.5	1,554.4	1,608.3	–1.1157	–1.2629	–1.338
4	2,084.3	2,104	2,111.7	–2.2787	–2.2987	–2.3085
5	2,674.7	2,689.7	2,695.8	–4.7534	–4.76	–4.7632
6	3,116.5	3,150.6	3,162.4	–6.1846	–6.2692	–6.3017

The varying friction coefficient with different material is plotted for better comparison between the GCI and aluminium composite as in Figure 9, the friction coefficient is taken as 0.1,0.3 and 0.4 as depicted in the figure.

Figure 9 Comparison of damping frequency for different friction coefficient with different material, where the GCI, Bi and Mono represent GCI, bimodal and monomodal, respectively (see online version for colours)

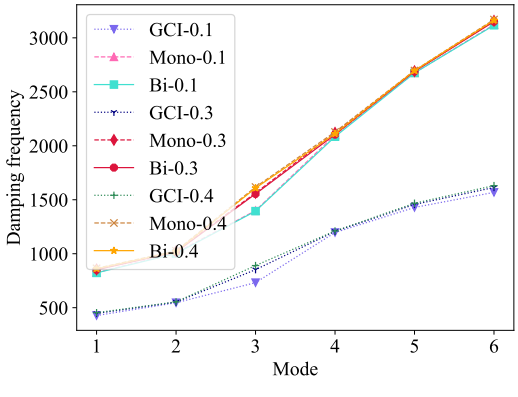

Figure 10 Comparison of stability for different friction coefficient with different material, where the GCI, Bi and Mono represent GCI, bimodal and monomodal, respectively (see online version for colours)

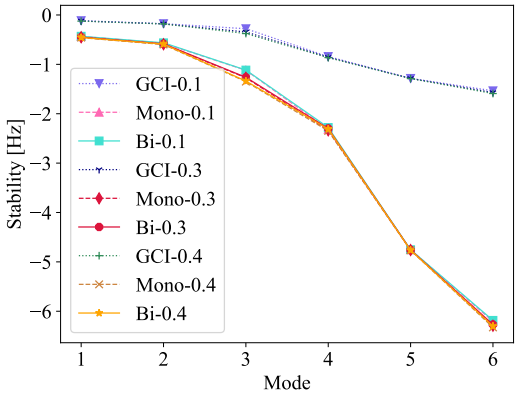

Figure 11 Comparison of damping factor for different friction coefficient with different material, where the GCI, Bi and Mono represent GCI, bimodal and monomodal, respectively (see online version for colours)

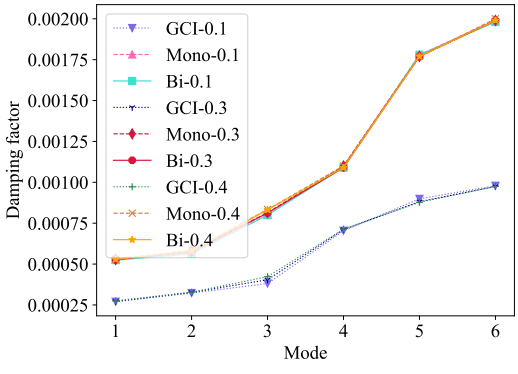

Figure 12 Comparison of logarithmic decrements for different friction coefficient with different material, where the GCI, Bi and Mono represent GCI, bimodal and monomodal, respectively (see online version for colours)

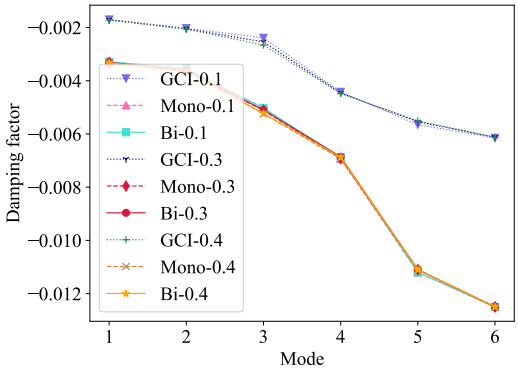

From the results the significant change in the damping frequency value at mode 3 indicates the influence of the varying friction coefficients affects the transverse bending mode on disc brake rotor. Similarly the stability (Figure 10), damping factor (Figure 11) and logarithmic decrements (Figure 12) are plotted to clarify the influence of the friction coefficient in the disc brake.

For the better understanding on the squeal noise induced because of the bending mode of the disc rotor, the first six modes are plotted for GCI, monomodal and bimodal as in Figure 13, 14 and 15, respectively.

Figure 13 Mode shape of the disc brake at 7,000 Hz and damping coefficient is 5%, (a) mode 1 (b) mode 2 (c) mode 3 (d) mode 4 (e) mode 5 (f) mode 6 (see online version for colours)

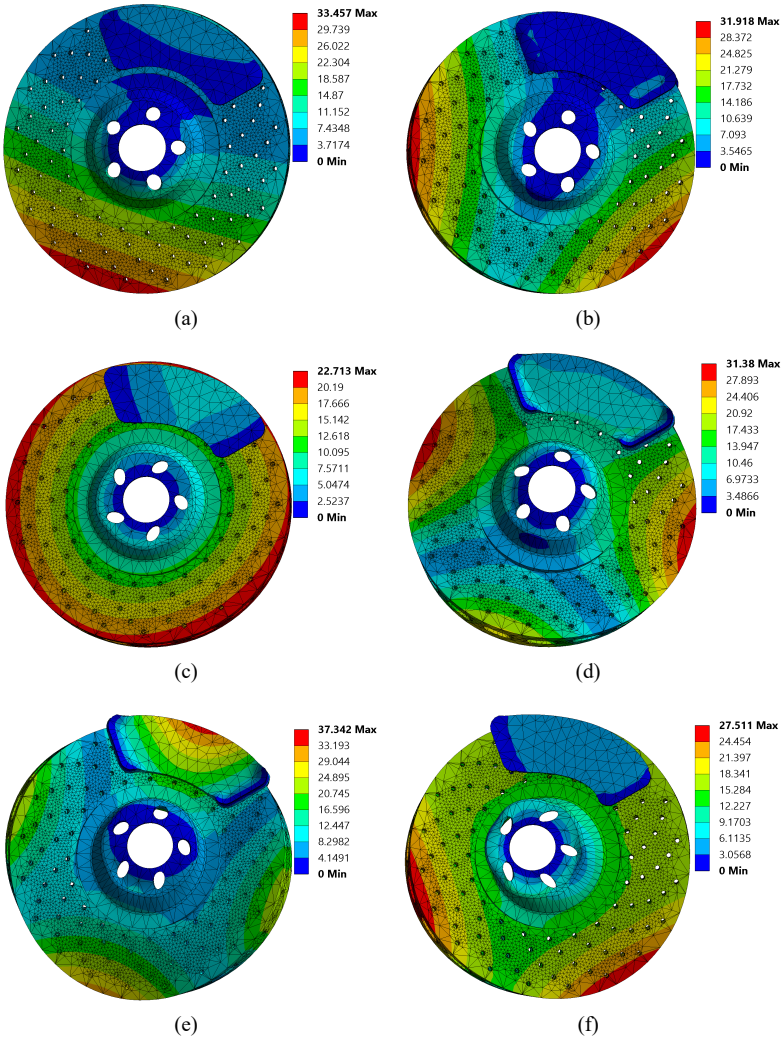

Figure 14 Mode shape for monomodal material subjected to 7,000 Hz with damping coefficient of 5%, (a) mode 1 (b) mode 2 (c) mode 3 (d) mode 4 (e) mode 5 (f) mode 6 (see online version for colours)

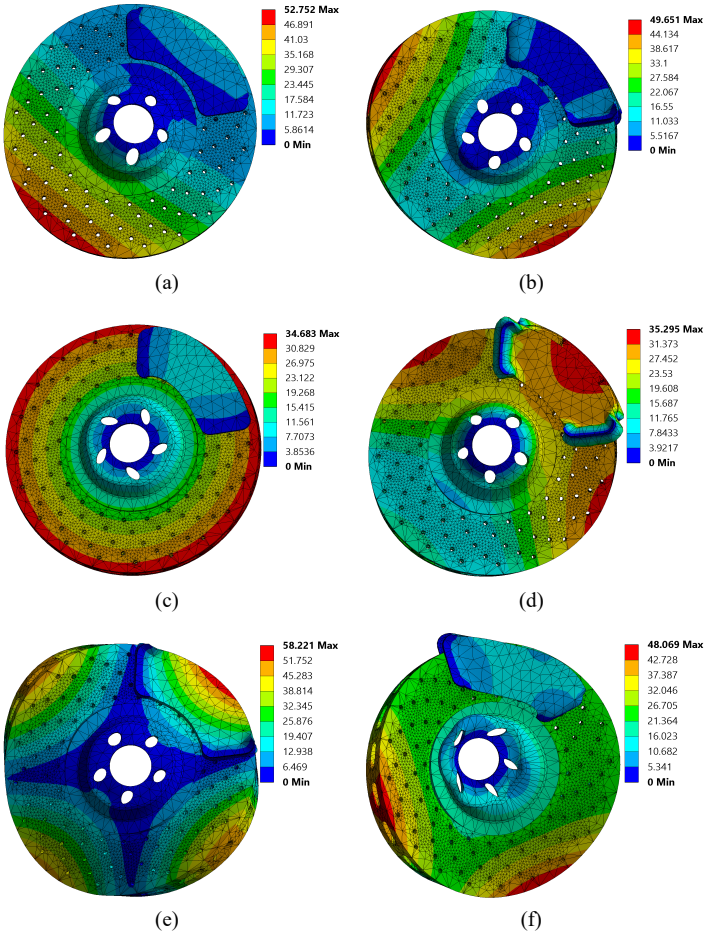

Figure 15 Mode shape for monomodal material subjected to 7,000 Hz with damping coefficient of 5%, (a) mode 1 (b) mode 2 (c) mode 3 (d) mode 4 (e) mode 5 (f) mode 6 (see online version for colours)

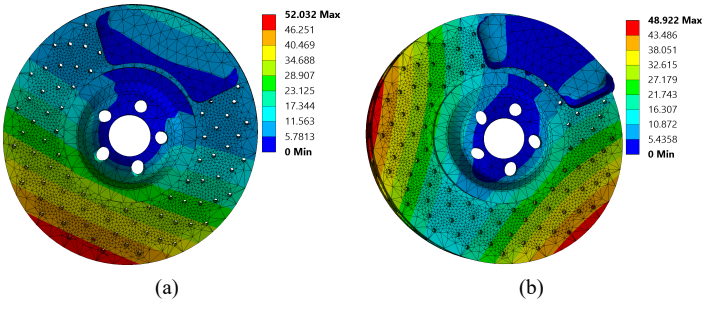

Figure 15 Mode shape for monomodal material subjected to 7,000 Hz with damping coefficient of 5%, (a) mode 1 (b) mode 2 (c) mode 3 (d) mode 4 (e) mode 5 (f) mode 6 (continued) (see online version for colours)

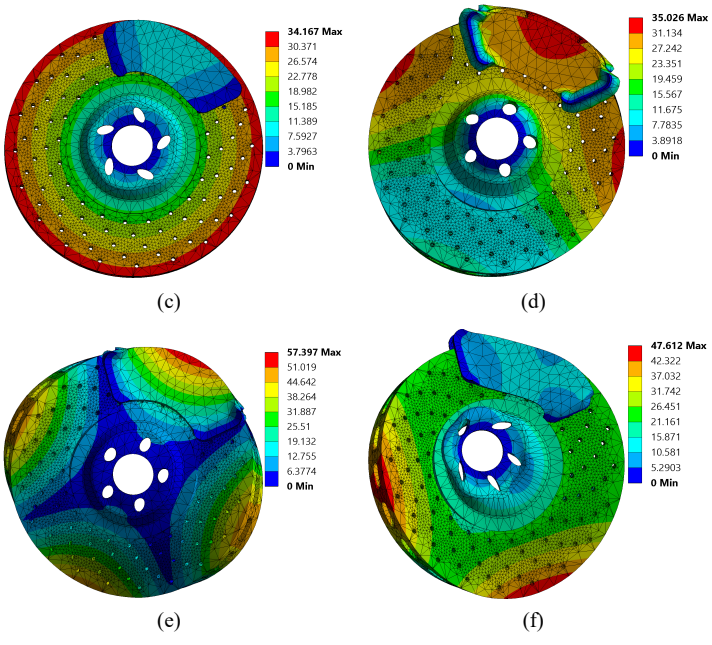

5 Conclusions

The influence of using different materials for the brake rotor to reduce squeal was investigated using CEA approach in Ansys Workbench. GCI was taken for the comparison since it is used commercially.

- the aluminium composite disc brake significantly affects the squeal noise in the brake rotor at higher frequency range
- the significant shift is close to 50% compared to the commercial disc brake rotor because of the change in the material property
- the influence of friction factor is analysed in detail, where the friction factor has more influence in particular damping frequency-bending mode
- reduction in weight and better performance with wear is an added advantage of aluminium composite disc brake rotor.

The detailed study on influence of damping coefficient and contact conditions is for future communication.

References

Adebisi, A., Maleque, M. and Rahman, M.M. (2011) 'Metal matrix composite brake rotor: historical development and product life cycle analysis', *International Journal of Automotive and Mechanical Engineering*, Vol. 4, No. 1, pp.471–480.

Denou, Y. and Nishiwaki, M. (2001) *First Order Analysis of Low Frequency Disk Brake Squeal*, SAE Technical Paper, No. 2001-01-3136.

Fosberry, R. and Holubecki, Z. (1959) *Interim Report on Disc Brake Squeal*, Technical Report, No. 1959/4, Motor Industry Research Association, Warwickshire, England.

Fosberry, R. and Holubecki, Z. (1961) *Disc Brake Squeal: Its Mechanism and Suppression*, Technical Report, No. 1961/1, Motor Industry Research Association, Warwickshire, England.

Giannini, O., Akay, A. and Massi, F. (2006) 'Experimental analysis of brake squeal noise on a laboratory brake setup', *Journal of Sound and Vibration*, Vol. 292, Nos. 1–2, pp.1–20.

Idusuyi, N., Babajide, I., Ajayi, O., Olugasa, T. et al. (2014) 'A computational study on the use of an aluminium metal matrix composite and aramid as alternative brake disc and brake pad material', *Journal of Engineering*, Vol. 2014, Article ID 494697, 6pp [online] https://doi.org/10.1155/2014/494697.

Kadu, N. and Vivekanandan, N. (2015) 'Numerical and experimental investigation of squeal noise generated in a disc brake system and reduction of it', *International Journal of Mechanical Engineering and Technology*, Vol. 6, No. 9, pp.10–16.

Kinkaid, N., O'Reilly, O.M. and Papadopoulos, P. (2003) 'Automotive disc brake squeal', *Journal of Sound and Vibration*, Vol. 267, No. 1, pp.105–166.

Liu, P., Zheng, H., Cai, C., Wang, Y., Lu, C., Ang, K. and Liu, G. (2007) 'Analysis of disc brake squeal using the complex eigenvalue method', *Applied Acoustics*, Vol. 68, No. 6, pp.603–615.

Mills, H. (1938) *Brake Squeal*, Report No. 9162 B, The Institution of Automobile Engineers.

Miracle, D. (2005) 'Metal matrix composites – from science to technological significance', *Composites Science and Technology*, Vol. 65, Nos. 15–16, pp.2526–2540.

Miranda, M.H.P., do Nascimento Rodrigues, R., de Araújo Bezerra, R., Lamary, P.M.C. and de Oliveira Neto, R.A. (2020) 'Numerical investigation of material properties and operating parameters effects in generating motorcycle break squeal using the finite element method', *Journal of the Brazilian Society of Mechanical Sciences and Engineering*, Vol. 42, No. 5, pp.1–16.

Montoya-Dávila, M., Pech-Canul, M.I., Escalera-Lozano, R. and Pech-Canul, M. (2010) 'Young's modulus of Al/SiC P/MgAl2O4 composites with different particle size distribution of reinforcements', *Matéria (Rio de Janeiro)*, Vol. 15, No. 2, pp.233–239.

Nilman, J. (2018) *Modeling and Simulation of Brake Squeal in Disc Brake Assembly* [online] http://kau.diva-portal.org/smash/get/diva2:1239833/FULLTEXT01.pdf.

Nouby, M., Sujatha, C. and Srinivasan, K. (2011) 'Modelling of automotive disc brake squeal and its reduction using rotor design modifications', *International Journal of Vehicle Noise and Vibration*, Vol. 7, No. 2, pp.129–148.

Pan, G., Zhang, X., Liu, P. and Chen, L. (2021) 'Impact analysis of contact symmetrical caliper structure on brake squeal', *Journal of Vibration and Control*, Vol. 27, Nos. 19–20, pp.2180–2191.

Qatu, M.S. (2012) 'Recent research on vehicle noise and vibration', *International Journal of Vehicle Noise and Vibration*, Vol. 8, No. 4, pp.289–301.

Qatu, M.S., Abdelhamid, M.K., Pang, J. and Sheng, G. (2009) 'Overview of automotive noise and vibration', *International Journal of Vehicle Noise and Vibration*, Vol. 5, Nos. 1–2, pp.1–35.

Sadagopan, P., Natarajan, H.K. and Kumar, P. (2018) 'Study of silicon carbide-reinforced aluminum matrix composite brake rotor for motorcycle application', *The International Journal of Advanced Manufacturing Technology*, Vol. 94, No. 1, pp.1461–1475.

Singla, M., Dwivedi, D.D., Singh, L., Chawla, V. et al. (2009) 'Development of aluminium based silicon carbide particulate metal matrix composite', *Journal of Minerals and Materials Characterization and Engineering*, Vol. 8, No. 6, p.455.

Triches Jr., M., Gerges, S. and Jordan, R. (2004) 'Reduction of squeal noise from disc brake systems using constrained layer damping', *Journal of the Brazilian Society of Mechanical Sciences and Engineering*, Vol. 26, No. 3, pp.340–348.